



THE UNIVERSITY *of* EDINBURGH

Edinburgh Research Explorer

Ultra-low temperature structure determination of a Mn-12 single-molecule magnet and the interplay between lattice solvent and structural disorder

Citation for published version:

Farrell, AR, Coome, JA, Probert, MR, Goeta, AE, Howard, JAK, Lemee-Cailleau, M-H, Parsons, S & Murrie, M 2013, 'Ultra-low temperature structure determination of a Mn-12 single-molecule magnet and the interplay between lattice solvent and structural disorder', *CrystEngComm*, vol. 15, no. 17, pp. 3423-3429.
<https://doi.org/10.1039/c3ce00042g>

Digital Object Identifier (DOI):

[10.1039/c3ce00042g](https://doi.org/10.1039/c3ce00042g)

Link:

[Link to publication record in Edinburgh Research Explorer](#)

Document Version:

Peer reviewed version

Published In:

CrystEngComm

Publisher Rights Statement:

Copyright © 2013 Royal Society of Chemistry. All rights reserved.

General rights

Copyright for the publications made accessible via the Edinburgh Research Explorer is retained by the author(s) and / or other copyright owners and it is a condition of accessing these publications that users recognise and abide by the legal requirements associated with these rights.

Take down policy

The University of Edinburgh has made every reasonable effort to ensure that Edinburgh Research Explorer content complies with UK legislation. If you believe that the public display of this file breaches copyright please contact openaccess@ed.ac.uk providing details, and we will remove access to the work immediately and investigate your claim.



Cite as:

Farrell, A. R., Coome, J. A., Probert, M. R., Goeta, A. E., Howard, J. A. K., Lemee-Cailleau, M-H., Parsons, S and Murrie, M. (2013). Ultra-low temperature structure determination of a Mn₁₂ single-molecule magnet and the interplay between lattice solvent and structural disorder†**. *CrystEngComm*, 15(17), 3423-3429.

Manuscript received: 09.01.2013; Accepted: 28.02.2013; Article published: 01.03.2013

Ultra-low temperature structure determination of a Mn₁₂ single-molecule magnet and the interplay between lattice solvent and structural disorder†**

Andrew R. Farrell,¹ Jonathan A. Coome,² Michael R. Probert,² Andr s E. Goeta,² Judith A. K. Howard,² Marie-H l ne Lem e-Cailleau,³ Simon Parsons^{4,*} and Mark Murrie^{1,*}

^[1]WestCHEM, School of Chemistry, University of Glasgow, Glasgow, UK.

^[2]Department of Chemistry, University of Durham, Durham, UK.

^[3]Institut Laue-Langevin, 38042 Grenoble, France.

^[4]EaStCHEM, School of Chemistry, Joseph Black Building, University of Edinburgh, West Mains Road, Edinburgh, EH9 3FJ, UK.

^[*]Corresponding author; e-mail: Mark.Murrie@glasgow.ac.uk, S.Parsons@ed.ac.uk

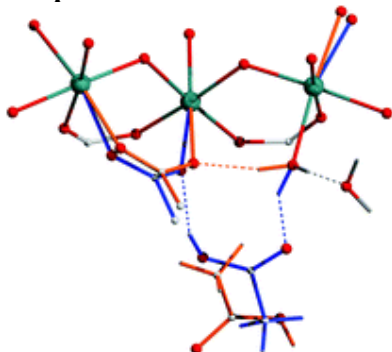
^[**]We thank STFC (CMSD08-04), The University of Glasgow and EPSRC for financial support, and the ILL for provision of neutron beam time. We also acknowledge useful comments on this work by G. J. McIntyre.

^[†]In memoriam Andr s E. Goeta.

Supporting information:

Electronic supplementary information (ESI) available: Crystallographic information files (CIFs) are available for each compound described herein as well as tables containing bond distances/tilt angles for 1, 2, 3. CCDC 916380–916382. For ESI and crystallographic data in CIF or other electronic format see <http://dx.doi.org/10.1039/C3CE00042G>

Graphical abstract:



Ultra-low Temperature Structure Determination of a Mn₁₂ Single-Molecule Magnet and the Interplay between Lattice Solvent and Structural Disorder†§

Andrew R. Farrell,^a Jonathan A. Coome,^b Michael R. Probert,^b Andr  s E. Goeta,^b Judith A. K. Howard,^b
Marie-H  l  ne Lem  e-Cailleau,^c Simon Parsons^{*d} and Mark Murrie^{*a}

Received (in XXX, XXX) Xth XXXXXXXXXX 20XX, Accepted Xth XXXXXXXXXX 20XX

DOI: 10.1039/b000000x

We have determined the ultra-low temperature crystal structure of the archetypal single-molecule magnet (SMM) [Mn₁₂O₁₂(O₂CMe)₁₆(H₂O)₄]·4H₂O·2MeCO₂H (**1**) at 2 K, by using a combination of single-crystal
X-ray and single-crystal neutron diffraction. This is the first structural study of any SMM in the same
temperature regime where slow magnetic relaxation occurs. We reveal an additional hydrogen bonding
interaction between the {Mn₁₂} cluster and its solvent of crystallisation, which shows how the lattice
solvent transmits disorder to the acetate ligands in the {Mn₁₂} complex. Unusual quantum properties
observed in **1** have long been attributed to disorder. Hence, we studied the desolvation products of **1**, in
order to understand precisely the influence of lattice solvent on the structure of the cluster. We present
two new axially symmetric structures corresponding to different levels of desolvation of **1**,
[Mn₁₂O₁₂(O₂CMe)₁₆(H₂O)₄]·4H₂O (**2**) and [Mn₁₂O₁₂(O₂CMe)₁₆(H₂O)₄] (**3**). In **2**, removal of acetic acid of
crystallisation largely resolves positional disorder in the affected acetate ligands, whereas removal of
lattice water molecules further resolves the acetate ligand disorder in **3**. Due to the absence of acetic acid
of crystallisation, both **2** and **3** have true, unbroken S₄ symmetry, showing for the first time that it is
possible to prepare fully axial Mn₁₂acetate analogues from **1**, via single-crystal to single-crystal
transformations.

Introduction

Single-molecule magnets (SMMs) are metal-organic clusters that
retain their magnetisation at low temperature after removal from a
magnetic field.¹ Although the first known SMM,
[Mn₁₂O₁₂(O₂CMe)₁₆(H₂O)₄]·4H₂O·2MeCO₂H (**1**), was reported in
1980, it was not identified as an SMM until much later.^{2, 3}
Subsequently there have been many SMMs reported, most based
on Mn^{III} chemistry⁴ although examples can be found that contain
other metal ions.^{5, 6} The slow relaxation of the magnetisation that
defines SMM behaviour occurs below a characteristic blocking
temperature, T_B. The highest reported T_B to date is ~13.9 K⁷,
besting the previous record of 8.3 K set only a few months prior.⁸
SMMs are of particular interest because of their potential for
storing and processing information at the molecular level.^{9, 10}
Recent work has focused strongly on integrating SMMs on
surfaces and devices,¹¹ including carbon nanotubes,¹² with the
aim of achieving a workable coupling between the nanoscale
units and the macroscopic world.

1 possesses an S=10 ground state and a significant axial
anisotropy, D ≈ - 0.5 cm⁻¹.^{13, 14} It has a blocking temperature of
approximately 3 K.¹⁵ The cluster consists of eight Mn^{III} centres
surrounding a central Mn^{IV}₄O₄ cubane, bridged by oxide and
acetate ligands. The interstitial voids are filled with water and
acetic acid of crystallisation, both of which take part in hydrogen
bonding to the complex. The acetic acid molecules are disordered
about a 2-fold rotation axis and lie directly between two adjacent
{Mn₁₂} clusters. The {Mn₁₂} cluster lies on a crystallographic S₄
axis and the eight Mn^{III} Jahn-Teller axes are approximately
aligned forming a magnetic easy axis.¹⁶

Scans of dc magnetisation vs. field show sharp steps in

hysteresis loops at well-defined field strengths.^{15, 17} The fast
relaxation at these steps is caused by resonant magnetic quantum
tunnelling (QTM). According to the fourfold symmetry of the
clusters, tunnelling is only permitted for even-to-even M_s
crossings, *i.e.* every fourth step is observable; however, QTM is
observed for all steps.

A previous structural study by Cornia *et al.* has suggested that
the two-fold disorder of the acetic acid of crystallisation leads to
six different isomers that make up **1**.^{16, 18} **1** contains 16 acetate
ligands, 4 of which are disordered about two positions (1 unique
ligand). This disorder is induced by disorder in the acetic acid of
crystallisation. There are four symmetry-related acetate ligands
that can be affected by this disorder and thus, six isomeric forms
exist for **1** that vary in the number of affected sites (n=0, 1, 2
(cis), 2 (trans), 3, 4).¹⁶ Axial symmetry is retained for the n=0 and
n=4 isomers but for the other four the symmetry is lowered. It has
been suggested that this permits a transverse anisotropy and thus,
provides an explanation for the odd-to-odd QTM steps in the
hysteresis loops.¹⁸ However, more recently published
measurements on a Mn₁₂ analogue (Mn₁₂-tBuAc)¹⁹ with full
crystallographic axial symmetry show that quantum tunnelling
occurs at odd-to-odd steps, even though this should be forbidden.
Similarly there is no easy explanation for the odd-to-even and
even-to-odd transitions observed for **1**. It was suggested that a
further consequence of the solvent disorder is that the molecular
easy axes are tilted discretely, inducing varying transverse
fields.²⁰ However, this explanation seems to be ruled out by the
previous observation of odd-to-odd transitions in both **1** and
Mn₁₂-tBuAc. Furthermore it is unlikely that dipolar coupling or
distributions of molecular environments are responsible either.¹⁹

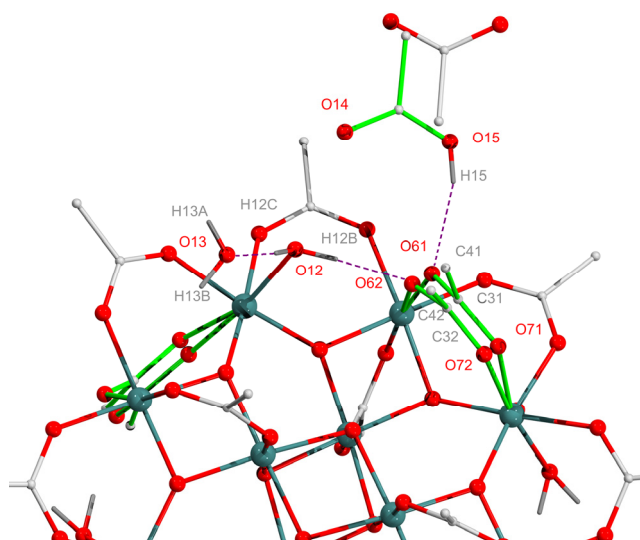


Fig. 1 Model showing disorder and hydrogen bonding proposed by Cornia *et al.* for $[\text{Mn}_{12}\text{O}_{12}(\text{O}_2\text{CMe})_{16}(\text{H}_2\text{O})_4] \cdot 4\text{H}_2\text{O} \cdot 2\text{MeCO}_2\text{H}$ (**1**). Hydrogen bonds from O12 to O62 and O13, and from O15 to O61 are indicated in purple. Most H atoms are omitted for clarity. Shown in green are acetic acid of crystallisation in the orientation in which it hydrogen bonds to the $\{\text{Mn}_{12}\}$ complex and both disorder components of the acetate ligand O6/O7/C3/C4 (denoted by the number '1' or '2' after the appropriate atom label, e.g. O61/O62, O71/O72).

Antisymmetric exchange has been proposed as a possible explanation, both for this system²¹ and for a similar observation in Ni_4 clusters.²²

In addition to stepped hysteresis loops below its blocking temperature, **1** also exhibits frequency-dependent ac susceptibility, a feature common to all single-molecule magnets due to their slow relaxation of magnetisation at ultra-low temperature. A curious feature of **1** compared to other SMMs is that there are two frequency-dependent peaks rather than the usual single peak: a large peak at 5–7 K and a much smaller peak at 2–3 K²³ due to slow-relaxing (SR) and fast-relaxing (FR) species respectively. The existence of two magnetic species has also been confirmed by inelastic neutron scattering (INS) measurements and it has been estimated that a typical distribution is 5% FR, 95% SR isomers.^{24, 25} It is unclear how these observations are related to the interesting quantum properties described above, or indeed the disorder observed crystallographically.

Previous attempts to understand the properties of **1** by structural correlation have utilised structural data measured at much higher temperatures than those at which slow magnetic relaxation is observed.^{16, 26} The lowest temperature at which structural data has previously been measured for **1** is 20 K by Langan *et al.*,²⁶ however disorder in the acetate ligands was not modelled. Thus, the best data that are currently available for **1** were measured at 83 K.¹⁶ It has been shown that application of pressure can change the structure of an analogue of the Mn_{12} family, $[\text{Mn}_{12}\text{O}_{12}(\text{O}_2\text{CCH}_2^t\text{Bu})_{16}(\text{H}_2\text{O})_4] \cdot \text{CH}_2\text{Cl}_2 \cdot \text{MeNO}_2$, such that its magnetisation relaxes much more slowly. High pressure crystallography reveals a structural change commensurate with the change in relaxation rates, specifically related to the switching of a misaligned Jahn-Teller axis into alignment with the magnetic

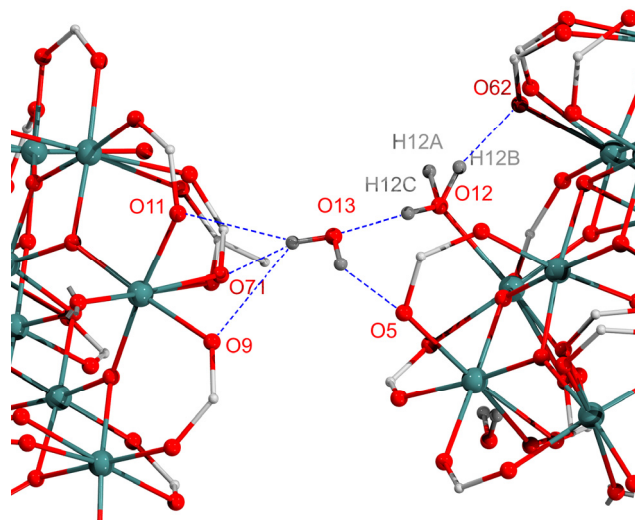


Fig. 2 Hydrogen bonding between $\{\text{Mn}_{12}\}$ clusters in compound **1** through water of crystallisation. Lattice acetic acid, some C atoms and most H atoms are omitted for clarity. The data is taken from our new 2 K structure determination.

easy axis.²⁷ Many molecular crystals undergo structural transformations upon cooling as well as under pressure,^{28–30} and it is possible that this could happen to **1** in a way that would influence the ultra-low temperature magnetic properties and quantum behaviour.

Results and discussion

Structural disorder at ultra-low temperature

Hitherto, no structural studies below 20 K²⁶ have been performed on **1**. At this temperature, the acetate ligand disorder was not observed and has only been modelled in a subsequent 83 K study.¹⁶ In order to rectify this, we carried out an ultra-low temperature structural study using both single-crystal X-ray and single-crystal neutron diffraction.[‡] We present the first structural data for an SMM measured at 2 K, *i.e.* in the same temperature regime in which hysteresis loops in *M* vs. *H* are observed. **1** is easy to handle and is the most-studied SMM in the literature. Furthermore, this study provides an opportunity to better understand the complex disorder inherent to the structure, which influences the observed quantum dynamics of the system.

The previous 20 K neutron study²⁶ performed on a partially deuterated crystal of **1** in conjunction with an 83 K X-ray study¹⁶ describes hydrogen bonding between the coordinated water molecule O12 and (i) the disordered acetate ligand [O12–H12B---O62] and (ii) the water of crystallisation [O12–H12C---O13] (figures 1, 2). The water of crystallisation itself acts as a hydrogen bond donor to O5 and three other possible acceptors O7, O9 and O11. The network of clusters is linked together through the solvent water in this way (figure 2). A hydrogen bond was also reported between the hydroxyl oxygen atom O15 in the solvent acetic acid and O61 of the disordered acetate ligand [O15–H15---O61] (figure 1).

We have solved the heavy-atom structure of **1** at 2 K by using single-crystal X-ray diffraction; hydrogen atoms involved in hydrogen-bonding were located by calculating a Fourier

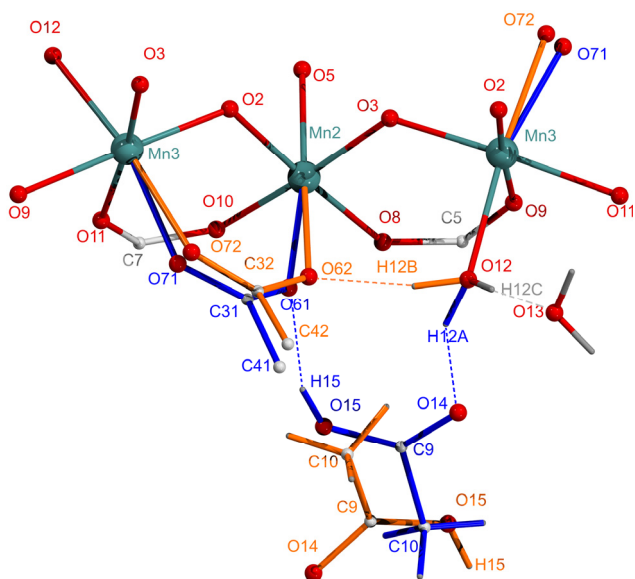


Fig. 3 New disorder model for compound **1** derived from our 2 K X-ray and neutron structure determination. Shown in blue are the positions of all affected atoms when the lattice acetic acid is facing towards the complex. Shown in orange are the positions of all affected atoms when the acetic acid is facing away from the complex. Most H atoms and some C atoms are omitted for clarity. Hydrogen bonds in the two disorder components are also indicated in their respective colours. Tilt angles (angle between S_4 axis and approximate Jahn-Teller axis) are as follows. Blue: O12-Mn3-O71 35.52(8)°, O5-Mn2-O61 15.35(8)°. Orange: O12-Mn3-O72 35.57(8)°, O5-Mn2-O62 9.73(7)°.

difference map from single-crystal neutron diffraction data at 2 K (see experimental details for further information). By doing so, we have found new evidence for an additional hydrogen-bonding interaction between the acetic acid of crystallisation and the water molecule O12 coordinated to Mn3 [O12-H12A---O14] (figure 3). This discovery neatly ties up a more complete understanding of hydrogen bonding in the region. We can expand on the previous model described by Cornia *et al.*¹⁶ as follows.

The whole disordered region can be thought of as two separate components each with 50% occupancy (figure 3); the occupancy is fixed by the location of the acetic acid of crystallisation on a 2-fold rotation axis. Each disorder component is linked with one orientation of the acetic acid. When the acid moiety is facing away from the cluster (shown in orange), there is an intramolecular hydrogen bond from coordinated water O12 to the adjacent acetate ligand O62. When the acid moiety is facing towards the cluster (shown in blue), there are two intermolecular hydrogen bonds from O15 to O61 and from O12 to O14. O61 and O62 are equivalent in that they are essentially the ‘same’ atom in the ligand but located in one of two different positions as dictated by either inter- or intra-molecular hydrogen bonding. The position of this atom influences the positions of the other atoms in the ligand: O71/O72, C31/C32 and C41/C42 and similar positional disorder is observed. It is clear that the disordered acetic acid is driving this disorder in the ligand atom positions and also in the nature of the hydrogen bonds. The half-occupied hydrogen atoms H12A and H12B uncovered by our neutron experiment confirm the nature of the hydrogen bonding in the region.

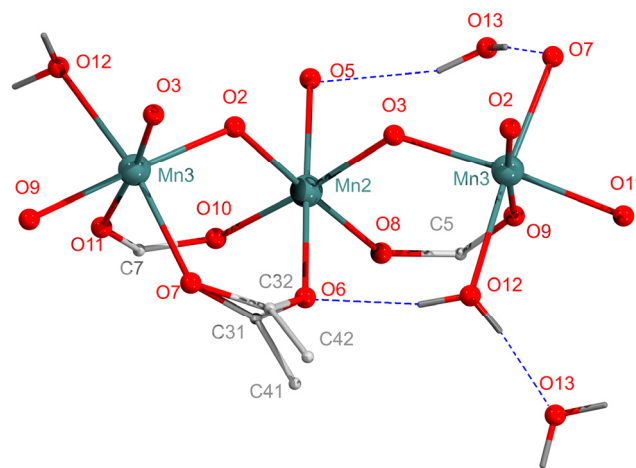


Fig. 4 Hydrogen bonding arrangement in $[\text{Mn}_{12}\text{O}_{12}(\text{O}_2\text{CMe})_{16}(\text{H}_2\text{O})_4] \cdot 4\text{H}_2\text{O}$ (**2**). Disorder in the positions of C atoms in the acetate ligand O6/O7/C3/C4 is still observed but the removal of acetic acid removes the disorder in the positions of atoms O6 and O7. Water of crystallisation is shown as an acceptor from O12 and a donor to O5 and O7.

The coordination environment of each Mn^{III} ion is broadly similar to that observed at higher temperatures. Around Mn2 there are four shorter bonds, ranging from 1.887(2) Å to 1.938(2) Å, and two longer axial bonds to O5 [2.224(2) Å] and O61/O62 [2.126(6)/2.247(5) Å]. This indicates a shortening of the axial elongation of approximately 0.12 Å when the acid moiety of the acetic acid of crystallisation is facing towards the cluster. This compares well with previously reported data by Cornia *et al.* for an 83 K X-ray structure (shortening of 0.09 Å).¹⁶

Mn3 also makes four shorter bonds, ranging from 1.889(2) Å to 1.979(3) Å, and two longer axial bonds to O12 [2.159(3) Å] and O71/O72 [2.126(6)/2.156(6) Å]. The solvent influence is evidently also felt in the coordination environment of Mn3, although the axial shortening of 0.03 Å is smaller. Interestingly, a lengthening of 0.05 Å for the Mn3-O71 vs. Mn3-O72 was reported previously.¹⁶ Angular distortions are not considerably different to those observed previously, being 13.9(2)° for O61-Mn2-O62 and 9.2(2)° for O71-Mn3-O72 [14.10(14)° and 6.8(3)° at 83 K]. The Jahn-Teller axes associated with both Mn2 and Mn3 are pseudo-aligned with the crystallographic c axis in either disorder component, despite small differences between the two. A full list of relevant bond distances is given in table S1. Although the Jahn-Teller axes are approximately aligned, they are not precisely aligned with the crystallographic c axis that is approximately equivalent to the molecular easy axis, given the tetragonal symmetry of the structure. The tilt angle (the angle between the Jahn-Teller axis and the easy axis) can be estimated by measuring the angle between the crystallographic c axis and the axis formed by the axially-elongated Mn-O bonds. The tilt angles associated with Mn3 (O12-O71/O72) are similar at 2 K to those measured at 83 K, while those associated with Mn2 (O5-O61/O62) show small but measureable differences. Angle at 2 K [Angle at 83 K¹⁸] for O12-O72: 35.57(8)° [35.46(7)°], O12-O71: 35.52(8)° [35.69(1)°], O5-O62: 9.73(7)° [10.41(5)°] and O5-O61: 15.35(8)° [16.17(8)°]. More interesting perhaps is to note the difference in tilt angle of over 5° between O5-O62 and O5-O61 at

either temperature (See ESI table 2 for a full comparison of tilt

angles). Another interesting comparison to make is the angle

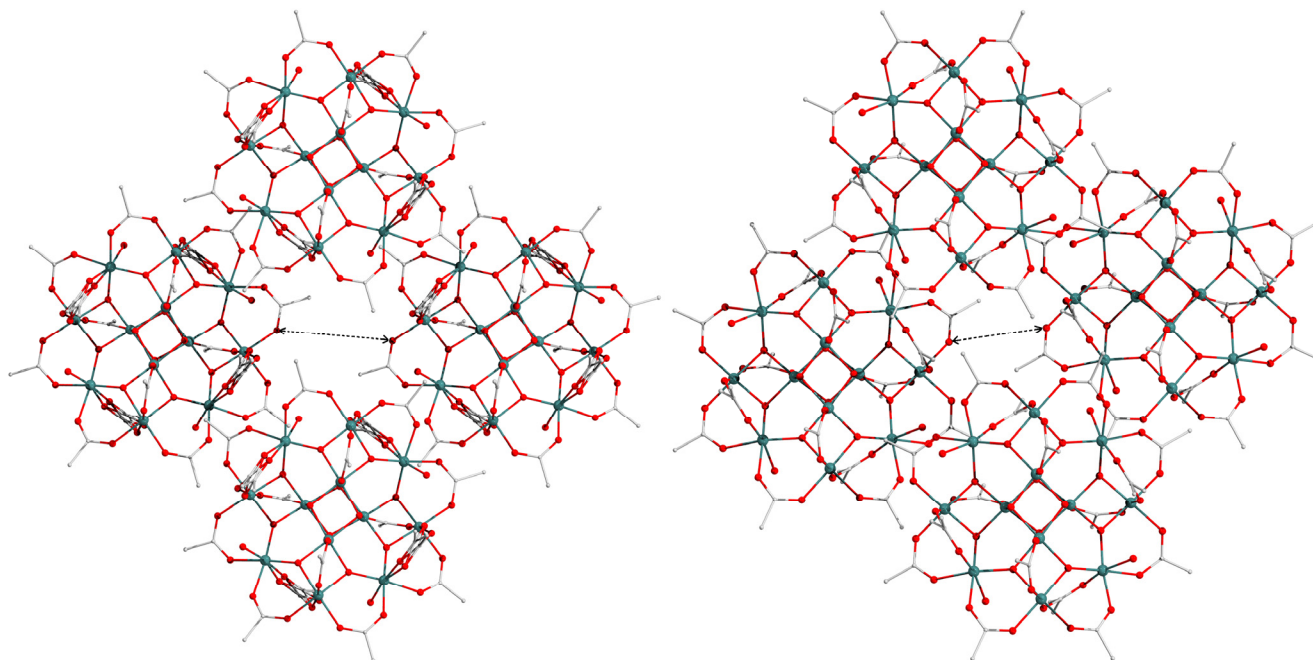


Fig. 5 Comparison of interstitial cavity size for compound **1** (left) and $[\text{Mn}_{12}\text{O}_{12}(\text{O}_2\text{CMe})_{16}(\text{H}_2\text{O})_4]$ (**3**) (right). All solvent of crystallisation is removed from the drawing of **1** for clarity. The marked cross-cavity distances are 5.8081(29) Å and 4.5114(30) Å respectively, showing a large reduction in cavity size upon full desolvation.

Table 1 Crystallographic data for **1**, **2** and **3**.

	1	2	3
Formula	$\text{C}_{36}\text{H}_{72}\text{Mn}_{12}\text{O}_{56}$	$\text{C}_{32}\text{H}_{64}\text{Mn}_{12}\text{O}_{52}$	$\text{C}_{32}\text{H}_{56}\text{Mn}_{12}\text{O}_{48}$
Moiety formula	$[\text{Mn}_{12}\text{O}_{12}(\text{OAc})_{16}(\text{H}_2\text{O})_4] \cdot 4\text{H}_2\text{O} \cdot 2\text{AcOH}$	$[\text{Mn}_{12}\text{O}_{12}(\text{OAc})_{16}(\text{H}_2\text{O})_4] \cdot 4\text{H}_2\text{O}$	$[\text{Mn}_{12}\text{O}_{12}(\text{OAc})_{16}(\text{H}_2\text{O})_4]$
M_w	2060.22	1939.96	1867.90
Crystal system	Tetragonal	Tetragonal	Tetragonal
Space group	$I-4$	$I-4$	$I-4$
a [Å]	17.1875(2)	17.235(4)	16.0506(12)
b [Å]	17.1875(2)	17.235(4)	16.0506(12)
c [Å]	12.1717(2)	12.038(3)	11.9067(12)
α [°]	90	90	90
β [°]	90	90	90
γ [°]	90	90	90
V [Å ³]	3595.64(8)	3576.0(14)	3067.4(4)
Z	2	2	2
T [K]	2.0(1)	100(2)	100(2)
Radiation	X-ray Mo (K_α) / neutron	X-ray Mo (K_α)	X-ray Mo (K_α)
λ [Å]	0.71073 / 'white'	0.71073	0.71073
D_c [g cm ⁻³]	1.903	1.802	2.022
μ [mm ⁻¹]	2.143	2.144	2.491
Meas./indep. refl.	24505/4861	10400/2469	18716/2694
R_{int}	0.0287	0.019	0.010
Obs. refl. [$I > 2\sigma(I)$]	4586	2351	2605
wR_2^a	0.0888	0.0329	0.0457
R_1^b	0.0366	0.0434	0.0234
Goodness of fit on F^2/F ^c	1.077	1.1297	0.9668
$\Delta\rho_{\text{max,min}}$ [e Å ⁻³]	0.826/-0.674	0.40/-0.29	0.06/-0.07

^a $wR_2 = \{\sum[w(F_o^2 - F_c^2)^2] / \sum[w(F_o^2)^2]\}^{1/2}$ on F^2 ; $wR_2 = \{\sum[w(F_o - F_c)^2] / \sum[w(F_o)^2]\}^{1/2}$ on F

^b $R_1 = \sum||F_o| - |F_c|| / \sum|F_o|$

^c Data for **1** were refined on F^2 ; data for **2** and **3** were refined on F .

between the planes formed by each ligand disorder component (*i.e.* the planes defined by O61/O71/C31/C41 and O62/O72/C32/C42 respectively, see figure 3). At 2 K this angle is just 6.1°, significantly lower than the 21.9° measured at 83 K.

This indicates that the atomic positions are significantly different at 2 K compared with 83 K.

Structural modification by removal of lattice solvent

It has long been postulated that the solvent acetic acid strongly influences the structure of the {Mn₁₂} cluster in **1**. In order to determine the true extent of this influence we carried out an experiment to desolvate crystals of **1**. Thermogravimetric analysis of **1** shows a large weight loss step at 383 K that is thought to correspond to loss of solvent acetic acid and water. Solvent was removed from **1** using a procedure[†] similar to that devised by Larionova *et al.*,³¹ who characterised the desolvated sample using powder X-ray diffraction and determined that the product retained the same space group and unit cell parameters as **1**. They claim that this product has both acetic acid and water removed, citing the previous TGA data and the experimentally observed Mn:C ratio as evidence³¹ but crucially they did not succeed in recording a single-crystal structure of the product.

Initial single-crystal X-ray analysis of our products indicated that there were two new types of crystal that, although visually identical, have different unit cells. Full structure determinations revealed the existence of the two new species [Mn₁₂O₁₂(O₂CMe)₁₆(H₂O)₄]·4H₂O (**2**) and [Mn₁₂O₁₂(O₂CMe)₁₆(H₂O)₄] (**3**). It should be noted that the Mn:C ratio for both these species is the same (1.72). Both crystallise in the same space group as **1**, *I*-4 (table 1). **2** has approximately the same unit cell lengths as **1** and is comprised of {Mn₁₂} clusters and lattice water in the same packing arrangement observed in **1**. The unit cell of **3** is approximately 14% smaller than that of the other two compounds and contains only {Mn₁₂} clusters. All Mn^{III} centres in both new structures **2** and **3** show the same pseudo-aligned axially-elongated Mn-O bonds observed in **1**. A comparison of bond distances between **1**, **2** and **3** is given in table S1. Intermolecular interactions are quite different in species **2** and **3**. As in **1**, **2** exhibits hydrogen bonding through lattice water O13 and the packing arrangement of {Mn₁₂} clusters is preserved (figure 4), with empty interstitial voids that were previously occupied by acetic acid. In **3** there is no lattice water to transmit hydrogen bonding and the clusters are closer together, maximising attractive dispersion forces. This close-packing could be responsible for the crystal retaining its crystallinity in spite of the removal of the relatively strong hydrogen bonds that previously held the structure together. The cavity that previously held lattice acetic acid is compressed and is too small to hold a molecule of this size (figure 5).

Removal of lattice acetic acid resolves the disorder in the positions of atoms O61/O62 and O71/O72. These can be modelled as single atoms O6 and O7 in both **2** and **3**, confirming that the lattice acetic acid is responsible for the disorder. C31/C32 is still disordered in **2** and C41/C42 is disordered in both **2** and **3**; this is unlikely to affect the Jahn-Teller axes on the Mn^{III} centres or indeed the quantum selection rules intrinsic to the molecular symmetry. The angles between the Jahn-Teller axes and the crystallographic *c* axis in **2** and **3** are broadly similar to those

observed previously, bearing in mind that these crystallographic data were collected at 100 K. [O12-O7, 34.13(6)° (**2**) and 36.38(4)° (**3**); O5-O6, 11.84(6)° (**2**) and 13.26(4)° (**3**)] (see table S2).

It is impossible to distinguish between crystals of **2** and **3** visually. Elemental analysis is consistent with the majority of crystals being species **2**, with a small amount of **3** present. Thus, we cannot claim to have produced pure samples of axially symmetric {Mn₁₂acetate} complexes. However we have shown that full removal of the acetic acid of crystallisation resolves the disorder in the O atoms of the acetate ligands, producing species that have true, unbroken *S*₄ symmetry. We expect **2** and **3** to exhibit similar QTM dynamics³²⁻³⁵ to other fully axial analogues in the Mn₁₂ family: Mn₁₂-tBuAc and Mn₁₂-BrAc. Hence, we are refining the single-crystal to single-crystal method used to produce species **2** and **3**, in order that we can selectively produce pure samples of either material for further study.

Conclusions

This study represents the first structural data collected for a single-molecule magnet, [Mn₁₂O₁₂(O₂CMe)₁₆(H₂O)₄]·4H₂O·2MeCO₂H (commonly Mn₁₂-acetate), at the same temperature as slow magnetic relaxation / hysteresis is observed, *i.e.* 2 K. We have described a more complete model of the disorder and hydrogen-bonding network inherent to the structure by using a combination of ultra-low temperature single-crystal X-ray and single-crystal neutron diffraction experiments. We have found an additional hydrogen bond in the disordered region that contributes to a clear understanding of how the lattice solvent transmits disorder to the {Mn₁₂} complex. A thorough comparison has been made between the structure measured at 2 K and the previously published data recorded at 83 K, revealing some interesting changes in the positions of each disordered component of the acetate ligands.

By studying the new desolvated species [Mn₁₂O₁₂(O₂CMe)₁₆(H₂O)₄]·4H₂O (**2**) and [Mn₁₂O₁₂(O₂CMe)₁₆(H₂O)₄] (**3**), prepared from **1** via single-crystal to single-crystal transformations, we have determined that disorder in the acetic acid of crystallisation is responsible for the positional disorder in an acetate ligand. Upon removal of the acetic acid of crystallisation, the positional disorder in the acetate ligand O6/O7/C3/C4 is largely resolved. An extended network is created by a series of hydrogen bonds between {Mn₁₂} clusters that take place through water of crystallisation. This network is preserved, even in the absence of acetic acid of crystallisation (in **2**), however when solvent water is removed (in **3**) the network is modified such that {Mn₁₂} clusters are significantly closer together. We plan to carry out further studies encompassing measurement of dc magnetisation vs. field, HF-EPR and NMR of **2** and **3** in order to understand their quantum behaviour in the context of **1** and other members of the Mn₁₂ family.

Acknowledgements

We thank STFC (CMSD08-04), The University of Glasgow and EPSRC for financial support, and the ILL for provision of neutron beam time. We also acknowledge useful comments on this work by G. J. McIntyre.

Notes and references

* $[\text{Mn}_{12}\text{O}_{12}(\text{O}_2\text{CMe})_{16}(\text{H}_2\text{O})_4]\cdot 4\text{H}_2\text{O}\cdot 2\text{MeCO}_2\text{H}$ (**1**) was synthesised as described previously.³⁶ A black crystal of **1** (size 0.1 x 0.1 x 1.0 mm) was mounted on a graphite rod and placed inside the cryostat of the XIPHOS diffractometer³⁷ (Mo K α radiation, $\lambda = 0.71073$ Å) at Durham University and cooled to 2 K. The system has a minimum operating temperature of 1.9 K, achieved using a modified two-stage closed-cycle refrigerator enhanced with an additional Joule-Thompson stage. Data were integrated using SAINT³⁸ and empirical absorption corrections using equivalent reflections were performed with the program SADABS.³⁹ Neutron Laue data were collected using the Very-Intense Vertical-Axis Laue Diffractometer at Institut Laue-Langevin, Grenoble.^{40, 41} The instrument has a minimum operating temperature of 1.5 K, achieved using a standard ILL 'orange' cryostat. A black crystal of **1** (size 0.2 x 0.2 x 1.0 mm) was mounted on a vanadium rod perpendicular to the incident beam. The sample used for the neutron study was not deuterated; indeed the negative scattering density from the hydrogen atoms was particularly advantageous in identifying their positions within the structure. 7 Laue patterns were collected for equally-spaced sample orientations, from 0° to 90° around the vertical rotation axis, covering a little more than a quadrant of reciprocal space. Cell parameters were taken from X-ray data at 2 K, and the Laue patterns were indexed using LAUEGEN. Background-corrected integrated intensities were extracted using ARGONNE_BOXES. Normalisation to a common wavelength was performed over the wavelength range 0.9-2.8 Å using LAUENORM.LAUEGEN⁴² and LAUENORM⁴³ are part of the Daresbury Laue Suite, while ARGONNE_BOXES is an in-house two-dimensional adaptation of the three-dimensional minimum $\sigma(I)/I$ routine.⁴⁴ X-ray data were used to determine cell parameters at 2 K as these are not derived from the Laue experiment. The heavy atom structure of **1** was solved and refined from X-ray data using the programs SHELXS-97⁴⁵ AND SHELXL-97⁴⁵ respectively. Hydrogen atoms in methyl groups were placed in calculated positions. This structural model was allowed to refine against the neutron data. Hydrogen atoms attached to coordinated and lattice water molecules, as well as the acidic hydrogen belonging to the solvent acetic acid, were found in a Fourier difference map calculated from the neutron data. The neutron data are especially useful in this regard due to the sensitivity of neutrons to hydrogen atoms. Finally the model was again refined against X-ray data with the located H atoms restrained. Crystal data for **1**: $\text{C}_{36}\text{H}_{72}\text{Mn}_{12}\text{O}_{56}$, $M = 2060.22$ g mol⁻¹, tetragonal, space group $I-4$, $a = 17.1875(2)$ Å, $c = 12.1717(2)$ Å, $V = 3595.64(8)$ Å³, $Z = 2$, $\rho_{\text{calcd}} = 1.903$ g cm⁻³, $\mu = 2.143$ mm⁻¹, 24505 reflections measured, 4861 independent reflections, $R_{\text{int}} = 0.0287$, $R_1 = 0.0366$, $wR_2 = 0.0888$ (4586 reflections with $I > 2\sigma(I)$), GOF on F^2 1.077, max/min residual electron density 0.826/-0.674 e Å⁻³.

Dissolution products $[\text{Mn}_{12}\text{O}_{12}(\text{O}_2\text{CMe})_{16}(\text{H}_2\text{O})_4]\cdot 4\text{H}_2\text{O}$ (**2**) and $[\text{Mn}_{12}\text{O}_{12}(\text{O}_2\text{CMe})_{16}(\text{H}_2\text{O})_4]$ (**3**) were prepared by heating a selection of crystals of **1** to 403 K for 2 hours under an N₂ flow. After cooling to room temperature the crystals had retained sufficient crystallinity in order to perform single-crystal X-ray diffraction measurements. Elemental analysis was performed on the bulk sample of crystals obtained directly from the dissolution process. Elemental analysis (%): calc'd for $[\text{Mn}_{12}\text{O}_{12}(\text{O}_2\text{CMe})_{16}(\text{H}_2\text{O})_4]\cdot 4\text{H}_2\text{O}$ ($\text{C}_{32}\text{H}_{64}\text{Mn}_{12}\text{O}_{52}$): C 19.81, H 3.33; found: C 19.96, H 3.08. Black crystals of **2** and **3** were coated in FOMBLIN Y and immediately cooled to 100(2) K on a Nonius Kappa CCD diffractometer⁴⁶ (Mo K α radiation, $\lambda = 0.71073$ Å). Data were integrated using DENZO⁴⁷ and empirical absorption corrections using equivalent reflections were performed with the program SADABS.³⁹ The structures were solved using the program Superflip⁴⁸ and refined using the least-squares refinement routine implemented within CRYSTALS.⁴⁹ Crystal data for **2**: $\text{C}_{32}\text{H}_{64}\text{Mn}_{12}\text{O}_{52}$, $M = 1939.96$ g mol⁻¹, tetragonal, space group $I-4$, crystal size 0.1 x 0.1 x 0.3 mm, $a = 17.235(4)$ Å, $c = 12.038(3)$ Å, $V = 3576.0(14)$ Å³, $Z = 2$, $\rho_{\text{calcd}} = 1.802$ g cm⁻³, $\mu = 2.144$ mm⁻¹, 10400 reflections measured, 2469 independent reflections, $R_{\text{int}} = 0.019$, $R_1 = 0.0434$, $wR_2 = 0.0329$ (2351 reflections with $I > 2\sigma(I)$), GOF on F 1.1297, max/min residual electron density 0.40/-0.29 e Å⁻³. Crystal data for **3**:

$\text{C}_{32}\text{H}_{56}\text{Mn}_{12}\text{O}_{48}$, $M = 1867.90$ g mol⁻¹, tetragonal, space group $I-4$, crystal size 0.1 x 0.1 x 0.3 mm, $a = 16.0506(12)$ Å, $c = 11.9067(12)$ Å, $V = 3067.4(4)$ Å³, $Z = 2$, $\rho_{\text{calcd}} = 2.022$ g cm⁻³, $\mu = 2.491$ mm⁻¹, 18716 reflections measured, 2694 independent reflections, $R_{\text{int}} = 0.010$, $R_1 = 0.0234$, $wR_2 = 0.0457$ (2605 reflections with $I > 2\sigma(I)$), GOF on F 0.9668, max/min residual electron density 0.06/-0.07 e Å⁻³.

^aWestCHEM, School of Chemistry, University of Glasgow, Glasgow, UK.

⁷⁵ E-mail: Mark.Murrie@glasgow.ac.uk

^bDepartment of Chemistry, University of Durham, Durham, UK

^cInstitut Laue-Langevin, 38042 Grenoble, France

^dSchool of Chemistry, University of Edinburgh, Edinburgh, UK. E-mail: S.Parsons@ed.ac.uk

⁸⁰ § In memoriam Andr  s E. Goeta

† Electronic Supplementary Information (ESI) available: Crystallographic Information Files (CIFs) are available for each compound described herein as well as tables containing bond distances/tilt angles for **1**, **2**, **3**. See DOI: 10.1039/b000000x/

⁸⁵

1. D. Gatteschi, R. Sessoli and J. Villain, *Molecular Nanomagnets*, OUP, Oxford, 2006.
2. A. Caneschi, D. Gatteschi, R. Sessoli, A. L. Barra, L. C. Brunel and M. Guillot, *J. Am. Chem. Soc.*, 1991, **113**, 5873.
3. R. Sessoli, H. L. Tsai, A. R. Schake, S. Y. Wang, J. B. Vincent, K. Folting, D. Gatteschi, G. Christou and D. N. Hendrickson, *J. Am. Chem. Soc.*, 1993, **115**, 1804.
4. C. J. Milios, A. Vinslava, W. Wernsdorfer, S. Moggach, S. Parsons, S. P. Perlepes, G. Christou and E. K. Brechin, *J. Am. Chem. Soc.*, 2007, **129**, 2754.
5. M. Murrie, *Chem. Soc. Rev.*, 2010, **39**, 1986.
6. G. Aromi and E. K. Brechin, in *Single-Molecule Magnets and Related Phenomena*, ed. R. E. P. Winpenny, Springer, 2006.
7. J. D. Rinehart, M. Fang, W. J. Evans and J. R. Long, *J. Am. Chem. Soc.*, 2011, **133**, 14236.
8. J. D. Rinehart, M. Fang, W. J. Evans and J. R. Long, *Nat. Chem.*, 2011, **3**, 538.
9. L. Bogani and W. Wernsdorfer, *Nature Mater.*, 2008, **7**, 179.
10. F. Troiani and M. Affronte, *Chem. Soc. Rev.*, 2011, **40**, 3119.
11. N. Domingo, E. Bellido and D. Ruiz-Molina, *Chem. Soc. Rev.*, 2012, **41**, 258.
12. M. del Carmen Gim  nez-L  pez, F. Moro, A. La Torre, C. J. G  mez-Garc  a, P. D. Brown, J. van Slageren and A. N. Khlobystov, *Nat. Commun.*, 2011, **2**, 407.
13. R. Sessoli, D. Gatteschi, A. Caneschi and M. A. Novak, *Nature*, 1993, **365**, 141.
14. I. Mirebeau, M. Hennion, H. Casalta, H. Andres, H. U. G  del, A. V. Irodova and A. Caneschi, *Phys. Rev. Lett.*, 1999, **83**, 628.
15. J. R. Friedman, M. P. Sarachik, J. Tejada and R. Ziolo, *Phys. Rev. Lett.*, 1996, **76**, 3830.
16. A. Cornia, A. C. Fabretti, R. Sessoli, L. Sorace, D. Gatteschi, A.-L. Barra, C. Daiguebonne and T. Roisnel, *Acta Cryst.*, 2002, **C58**, m371.
17. L. Thomas, F. Lioni, R. Ballou, D. Gatteschi, R. Sessoli and B. Barbara, *Nature*, 1996, **383**, 145.
18. A. Cornia, R. Sessoli, L. Sorace, D. Gatteschi, A. L. Barra and C. Daiguebonne, *Phys. Rev. Lett.*, 2002, **89**, 257201.
19. W. Wernsdorfer, M. Murugesu and G. Christou, *Phys. Rev. Lett.*, 2006, **96**, 057208.
20. S. Takahashi, R. S. Edwards, J. M. North, S. Hill and N. S. Dalal, *Phys. Rev. B*, 2004, **70**, 094429.

21. H. De Raedt, S. Miyashita, K. Michielsen and M. Machida, *Phys. Rev. B*, 2004, **70**, 064401.
22. N. Kirchner, J. van Slageren, B. Tsukerblat, O. Waldmann and M. Dressel, *Phys. Rev. B*, 2008, **78**, 094426.
- 5 23. M. Evangelisti, J. Bartolome and F. Luis, *Solid State Commun.*, 1999, **112**, 687.
24. M. Evangelisti and J. Bartolomé, *J. Magn. Magn. Mater.*, 2000, **221**, 99.
25. O. Waldmann, G. Carver, C. Dobe, A. Sieber, H. U. Güdel and H. Mutka, *J. Am. Chem. Soc.*, 2007, **129**, 1526.
- 10 26. P. Langan, R. Robinson, P. J. Brown, D. Argyriou, D. Hendrickson and G. Christou, *Acta Cryst.*, 2001, **C57**, 909.
27. P. Parois, S. A. Moggach, J. Sanchez-Benitez, K. V. Kamenev, A. R. Lennie, J. E. Warren, E. K. Brechin, S. Parsons and M. Murrie, *Chem. Commun.*, 2010, **46**, 1881.
- 15 28. J.-F. Bardeau, A. Bulou, W. T. Klooster, T. F. Koetzle, S. Johnson, B. Scott, B. I. Swanson and J. Eckert, *Acta Cryst.*, 1996, **B52**, 854.
29. D.-H. Wu, L. Jin and Y. Zhang, *Inorg. Chem. Commun.*, 2012, **23**, 117.
- 20 30. B. A. Zakharov, E. A. Losev, B. A. Kolesov, V. A. Drebuschak and E. V. Boldyreva, *Acta Cryst.*, 2012, **B68**, 287.
31. J. Larionova, R. Clerac, B. Boury, J. Le Bideau, L. Lecren and S. Willemin, *J. Mater. Chem.*, 2003, **13**, 795.
- 25 32. S. Hill, N. Anderson, A. Wilson, S. Takahashi, K. Petukhov, N. E. Chakov, M. Murugesu, J. M. North, E. d. Barco, A. D. Kent, N. S. Dalal and G. Christou, *Polyhedron*, 2005, **24**, 2284.
33. S. Hill, N. Anderson, A. Wilson, S. Takahashi, N. E. Chakov, M. Murugesu, J. M. North, N. S. Dalal and G. Christou, *J. Appl. Phys.*, 2005, **97**, 10M510.
- 30 34. N. E. Chakov, S.-C. Lee, A. G. Harter, P. L. Kuhns, A. P. Reyes, S. O. Hill, N. S. Dalal, W. Wernsdorfer, K. A. Abboud and G. Christou, *J. Am. Chem. Soc.*, 2006, **128**, 6975.
- 35 35. G. Redler, C. Lampropoulos, S. Datta, C. Koo, T. C. Stamatatos, N. E. Chakov, G. Christou and S. Hill, *Phys. Rev. B*, 2009, **80**, 094408.
36. T. Lis, *Acta Cryst.*, 1980, **B36**, 2042.
37. M. R. Probert, C. M. Robertson, J. A. Coome, J. A. K. Howard, B. C. Michell and A. E. Goeta, *J. Appl. Cryst.*, 2010, **43**, 1415.
- 40 38. Bruker, *SAINT*, 2007, Bruker AXS Inc., Madison, Wisconsin, USA.
39. G. M. Sheldrick, *SADABS*, 1996, University of Göttingen, Germany.
40. C. Wilkinson, J. A. Cowan, D. A. A. Myles, F. Cipriani and G. J. McIntyre, *Neutron News*, 2002, **13**, 37.
41. G. J. McIntyre, M.-H. Lemée-Cailleau and C. Wilkinson, *Physica B: Condensed Matter*, 2006, **385-386**, 1055.
- 45 42. J. W. Campbell, Q. Hao, M. M. Harding, N. D. Nguti and C. Wilkinson, *J. Appl. Cryst.*, 1998, **31**, 496.
43. J. W. Campbell, J. Habash, J. R. Helliwell and K. Moffat, in *Information Quarterly for Protein Crystallography No. 18*, SERC Daresbury Laboratory, Warrington, England, 1986, p. 23.
- 50 44. C. Wilkinson, H. W. Khamis, S. R. F. D. and G. J. McIntyre, *J. Appl. Cryst.*, 1988, **21**, 471.
45. G. M. Sheldrick, *Acta Cryst.*, 2008, **A64**, 112.
- 55 46. Nonius, *COLLECT*, 1998, Nonius BV, Delft, The Netherlands.
47. Z. Otwinowski and W. Minor, *Macromolecular Crystallography, Part A*, Academic Press, New York, 1997.
48. L. Palatinus and G. Chapuis, *J. Appl. Cryst.*, 2007, **40**, 786.
49. P. W. Betteridge, J. R. Carruthers, R. I. Cooper, K. Prout and D. J. Watkin, *J. Appl. Cryst.*, 2003, **36**, 1487.